Nanocomposites of Poly(methyl methacrylate) and Organically Modified Layered Silicates by Melt Intercalation

Zhiqi Shen,[1] George P. Simon,[2] Yi-Bing Cheng[2]

[1]*Manufacturing and Infrastructure Technology, Commonwealth Scientific and Research Organization, P.O. Box 56, Highett, Victoria 3190, Australia*
[2]*School of Physics and Materials Engineering, Monash University, Victoria 3800, Australia*

Received 31 July 2003; accepted 20 November 2003

ABSTRACT: Polymer-layered silicate nanocomposites of poly(methyl methacrylate) (PMMA) and an organically modified silicate [tetraallkyl ditallow ammonium bentonite (B34)] system prepared via melt intercalation were studied. The saturation ratio of PMMA to B34 was 25:75 (w/w), as determined by dynamic mechanical thermal analysis, differential scanning calorimetry, and X-ray diffraction. The interaction between PMMA and B34 was detected by Fourier transform infrared spectrometry, which showed two new absorption bands of PMMA/B34 hybrids in comparison with unannealed physical mixtures of PMMA and B34. The degradation temperature of the PMMA/B34 hybrids was 26°C higher than that of neat PMMA according to thermogravimetric analysis, the thermal stability of the hybrids having been enhanced. The glass-transition temperature of excess PMMA remaining outside the clay galleries was about 12–19°C higher than that of neat PMMA. A structural model of the hybrid was also presented. It involves some PMMA chains diffusing into the gallery of B34 and expanding it by 6.8 Å and some penetrating and interacting with the organic chains of the modified cations. Some of the PMMA chains partly contained inside the clay layers were entangled with those remaining outside when PMMA in excess of the saturation ratio was used. © 2004 Wiley Periodicals, Inc. J Appl Polym Sci 92: 2101–2115, 2004

Key words: nanocomposites; clay; melt structure

INTRODUCTION

Polymer-layered silicate nanocomposites have been the subject of much industrial and academic research interest because they promise superior or unique properties in comparison with those of the original polymers, including increased modulus, decreased thermal expansion coefficient, increased heat distortion temperature, reduced gas permeability, increased solvent resistance, enhanced ionic conductivity, low flammability, and better fire-retardant properties. In particular, melt intercalation (as opposed to solution or polymerization intercalation) remains an attractive method of introducing the polymer chains into the silicate galleries. Nylon,[1] poly(ethylene oxide) (PEO),[2] and polystyrene (PS)[3] remain the most commonly examined thermoplastic materials by melt intercalation. Poly(methyl methacrylate) (PMMA)/clay nanocomposites have been reported but mainly in polymer-rich clay-intercalated or -exfoliated PMMA composites,[4,5] most PMMA/clay nanocomposites being made by the *in situ* polymerization route[6,7] (in which the monomer and silicate are mixed and the monomer is subsequently polymerized.). A PMMA/sodium montmorillonite (MMT) intercalated nanocomposite, made through the emulsion polymerization of methyl methacrylate (MMA) monomer and MMT, has also been reported in detail, and both the thermal stability and tensile properties have been substantially enhanced.[8] The thermal and thermomechanical properties of exfoliated PMMA/MMT nanocomposites have been studied,[5,9–11] and the glass-transition temperature (T_g), thermal stability, and flame retardancy have been increased.

In this investigation, the intercalation of PMMA into an unmodified clay (MMT) or an organically modified bentonite [tetraallkyl ditallow ammonium bentonite (B34)] via the melt intercalation method for clay-rich materials was attempted. The structural characteristics and thermal properties of the PMMA/B34 nanocomposites were investigated. Evidence of PMMA melt intercalation and the saturation ratio of PMMA in B34, in cases in which nanocomposites were formed, was determined from X-ray diffraction (XRD), infrared (IR) spectroscopy, and thermal analysis techniques [differential scanning calorimetry (DSC), thermogravimetric analysis (TGA), and dynamic mechanical thermal analysis (DMTA)]. The saturation ratio (the amount of the polymer required to fill the clay galleries before

Correspondence to: G. P. Simon (george.simon@spme.monash.edu.au).

Journal of Applied Polymer Science, Vol. 92, 2101–2115 (2004)

TABLE I
Molecular Weight, Tacticity, and Polydispersity of Methacrylate Polymers

Material	Notation	M_n	M_w	Polydispersity
a-PMMA	424	7,580	13,781	1.81
i-PMMA	689	40,887	79,512	1.95

a = atactic; i = isotactic; M_n = number-average molecular weight; M_w = weight-average molecular weight.

there is an excess) is rarely reported in such nanocomposite systems. A structural model for PMMA incorporated into B34 by melt intercalation is also proposed.

EXPERIMENTAL

The silicate materials used were MMT and an organically modified bentonite (B34). The tallow unit was an alkyl chain of various lengths ($C_{14} \approx 5$ wt %, $C_{16} \approx 25$ wt %, and $C_{18} \approx 70$ wt %). MMT was obtained from the Source Clay Minerals Repository (Univ. of Missouri) and was used after being heated at 250°C for 300 min to reduce the amount of intercalated water. B34 is made from bentonite cation-exchanged with the ammonium organoion mentioned previously, and it is a commercial material from Rheox (New Elementis, Hightstown, NJ) and was used as received. The polymers used were atactic PMMA 424 and isotactic PMMA 689; the details are summarized in Table I.

Nanocomposites of the PMMA/B34 system were prepared via the quiescent-heated, melt intercalation method.[3] Powders with different weight ratios of the polymer to silicate (up to 30:70) were mechanically mixed with an agate mortar and pestle and then formed into disks with a hydraulic press at a pressure of 70 MPa. The silicate was usually in excess concentrations to allow the study of intercalation (as opposed to exfoliation). Intercalation was accomplished through the annealing of the pressed disks in an electrical resistance furnace *in vacuo* at a suitable temperature for 8 h. The annealing temperature was about 120°C higher than the polymer T_g, as measured by the DSC technique. The temperature was 210°C for PMMA 424 ($T_g \sim 94$°C) and 160°C for PMMA 689 ($T_g \sim 46$°C). The annealing temperatures and the times at these isothermal temperatures were designed to encourage full melt intercalation.

An important way of monitoring the introduction of polymer chains into silicate is XRD. Diffraction patterns on powdered samples were obtained on a Rigaku Geigerflex X-ray diffractometer (The Woodlands, TX) with nickel-filtered Cu Kα radiation at a scanning speed of 1°/min and a step of 0.05°. To study changes in the polymer chain environment, we used Fourier transform infrared (FTIR) spectroscopy. The spectra were collected with a PerkinElmer 1600 (Boston, MA) from 400 to 4000 cm^{-1} with a nominal resolution of 2 cm^{-1}. For each spectrum, 64 runs were collected and averaged. The specimens were made through the addition of 1% of the sample powder to KBr powder, which was then pressed into a disc 13 mm in diameter and 1–2 mm thick *in vacuo*.

DSC was performed on a PerkinElmer DSC-7 differential scanning calorimeter. Samples of approximately 10 mg were measured in an aluminum pan; both the sample and reference chamber with an empty pan were heated at 10°C/min from 20 to 160°C. TGA was performed on a Setaram TG-DTA 92 instrument (Calvire, France) at a heating rate of 10°C/min from 50 to 1000°C in a flow of air or nitrogen. DMTA was carried out with a PerkinElmer DMA7 instrument and penetration probe geometry; the oscillating probe tip was placed directly on the surface of the compressed unannealed or annealed sample biscuit, helium being flushed at a rate of 40 mL/min. The temperature was scanned from 20 to 150°C at a rate of 5°C/min, and the applied frequency was 1 Hz. The sample was approximately a 3–4-mm cube. The glass transition measured by DMTA was defined as the peak temperature of the maximum of the loss modulus plot.

The density data in this work were obtained on a Micrometritics AccuPyc 1330 helium pycnometer (Norcross, GA). In the pycnometer, the volume change was determined from pressure changes caused by the introduction of a sample of known weight. The samples were fine powders and approximately 4 g. Fifteen runs were obtained for the calculation of the density for each sample and averaged.

RESULTS AND DISCUSSION

Evidence of PMMA melt intercalation

The intercalation of PMMA into either MMT or B34 was attempted via melt intercalation. Because PMMA is an amorphous polymer, no XRD peak corresponding to the polymer occurs, and the XRD pattern of a mixture of PMMA and MMT or B34 yields only the diffraction peaks of MMT or B34 and any impurities (mainly quartz) in the clay. The only indication of intercalation from XRD would be a shift in the (00l) peaks from their original positions for pristine layered silicate to lower 2θ angle positions for the final, intercalated hybrid. Figure 1(a,b) shows XRD patterns of a mixture of PMMA 424 and MMT (30:70) before and after annealing, respectively. There is no shift of the (00l) peaks to lower 2θ angles in the sample after annealing. This is clear evidence that the PMMA materials used were not able to diffuse into unmodified MMT via melt intercalation.

Although the PMMA samples used were not able to intercalate into MMT via melt intercalation, organi-

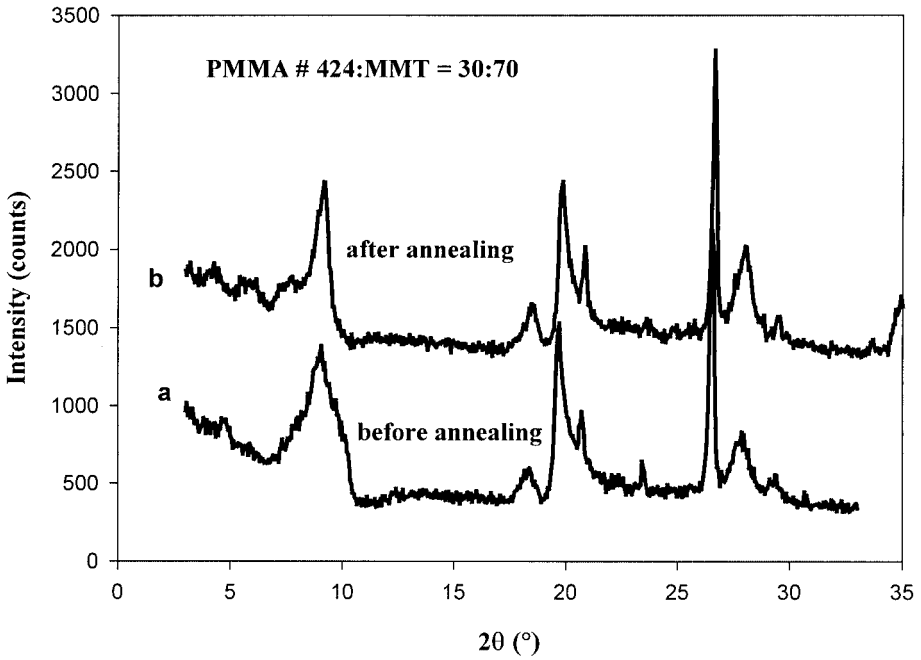

Figure 1 XRD patterns of a mixture of PMMA 424 and MMT (30:70) (a) before and (b) after annealing.

cally modified layered silicates such as B34 did show such behavior. Figure 2 shows the XRD patterns of both PMMA 424/B34 and PMMA 689/B34 samples after annealing and a physical mixture of PMMA 424 and B34 before annealing. The *d*-spacing of (001) in B34 is about 30.0 Å [Fig. 2 (a)]. The *d*-spacing of the (001) peak is 36.8 Å for the samples of 30:70 PMMA 424/B34 and 30:70 PMMA 689/B34, as shown in Figure 2(b,c). A series of new (00*l*) peaks also appeared and shifted to lower 2θ angles from the original peak positions for B34, although the peaks, which belong to (*hk*0) planes, did not change their positions after intercalation. This indicates that these two PMMAs (a-PMMA 424 and i-PMMA 689) entered the galleries of

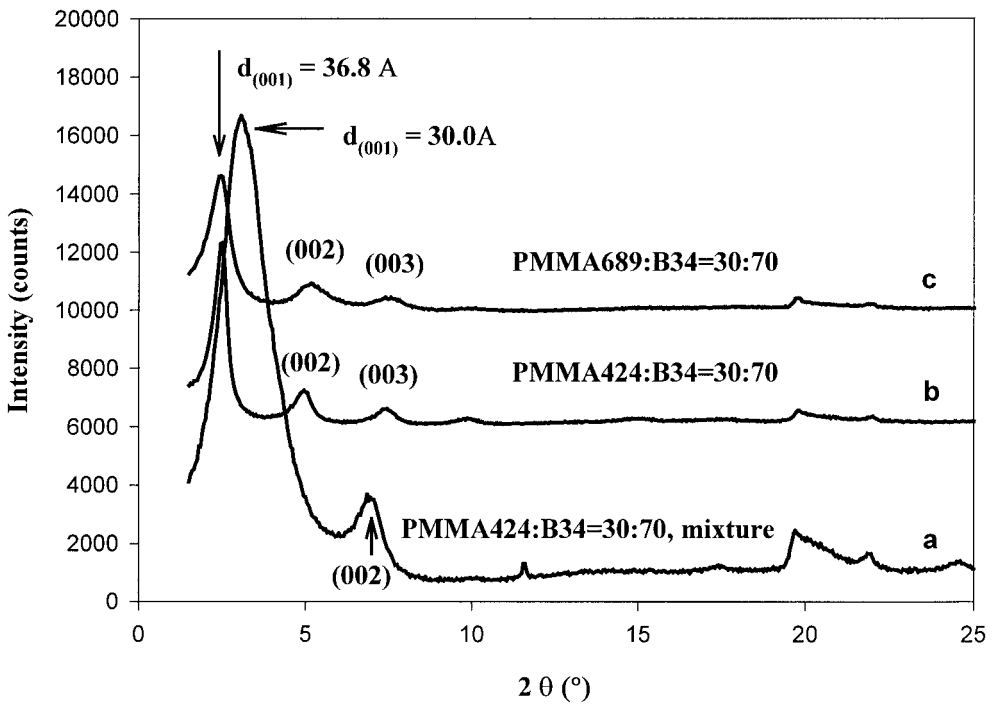

Figure 2 XRD patterns for both types of PMMA/B34 samples.

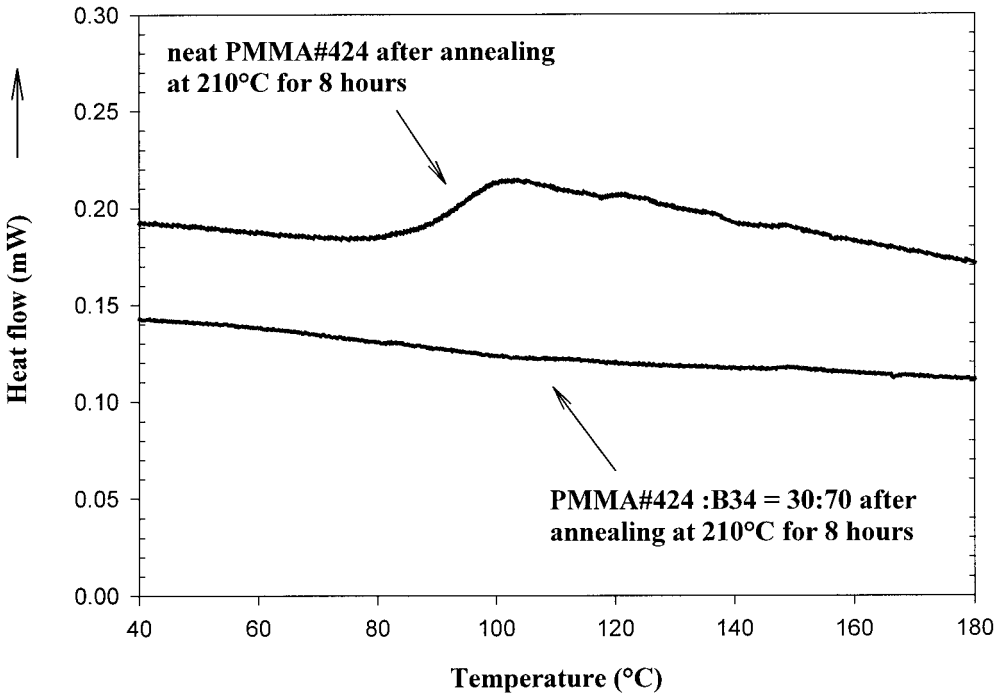

Figure 3 DSC traces of neat PMMA 424 and a sample of 30/70 PMMA 424/B34 after annealing.

B34, expanding the gallery distance by about 6.8 Å. a-PMMA 424 and i-PMMA 689 could readily intercalate into B34. In contrast, some other atactic PMMAs with higher molecular weights or higher T_g's (details not shown here) were not able to melt-intercalate into B34. The annealing temperatures required for intercalation would become too high and lead to degradation of B34 (the degradation temperature of alkyl ammonium ions of B34 is about 220–230°C) before intercalation.[12]

Evidence of the ability of the two PMMA samples to melt-intercalate can also be obtained from DSC results. Figure 3 shows DSC traces of neat PMMA 424 and a 30:70 mixture of PMMA 424 and B34 after annealing at 210°C for 8 h. T_g of PMMA 424 could be clearly seen in the neat sample, but it was not apparent in the sample of 30:70 PMMA 424/B34 after annealing. PMMA 689 shows similar behavior in the DSC traces. Once all PMMA went into the silicate galleries, the glass transition could no longer be seen. The same phenomenon has been reported for other polymer/clay systems, such as a PS/OMTS (organically modified mica-type silicate) system with 25% PS[13] and a PEO/MMT system with 20–25% PEO.[14] The absence of a glass transition is an important indication of PMMA intercalation.

In summary, it is clear that the lower molecular weight PMMA samples were able to melt-intercalate into the organoion-treated bentonite, but not into MMT alone. In our previous work with PEO, it was able to enter both untreated (MMT) and treated silicates (B34),[15] but this is uncommon, most polymers usually being unable to melt-intercalate into non-organoion-layered silicates. In that work, we did find, however, that the rate of melt intercalation of PEO was enhanced by the presence of organoions in the PEO system.[16]

Saturation ratio of PMMA to B34

Because of the limited space in which the silicate interlayer can expand via melt intercalation, there should be a saturation limit of the amount of polymer that can be intercalated into the layered silicates. This saturation ratio of polymer to layered silicate is important in both scientific research and industrial applications. There is a majority clay phase when the polymer is less than the saturation limit, as opposed to the situation when there is excess polymer and exfoliation may be possible. If the system were required to achieve exfoliation of silicate layers in a polymeric matrix, it would need a higher polymer concentration than that defined by the saturation limit. The saturation ratio of polymer to silicate is thus an important technical parameter in the design of weight ratios required in any real industrially compatible process. Conceptually, the density of the polymer in the galleries can also be calculated if the saturation ratio is known, and this could help us to further understand the conformation of the polymer in galleries. Because PMMA is an amorphous polymer, the reflections of crystallinity on peaks in XRD or the melting peak in

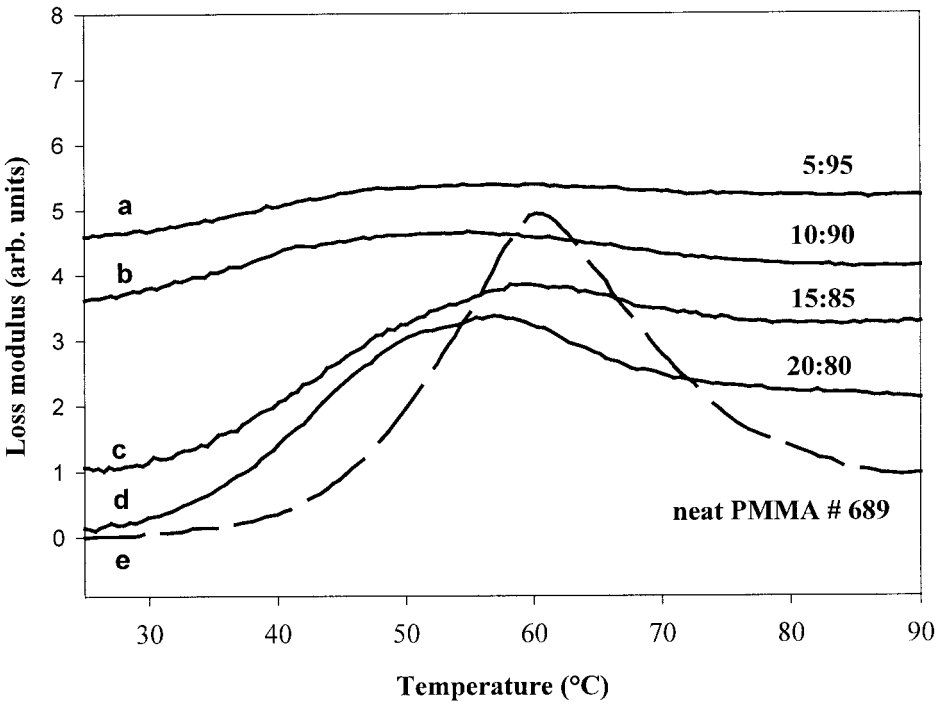

Figure 4 Loss modulus versus temperature for the PMMA 689/B34 system before annealing: (a) 5:95 PMMA 689/B34, (b) 10:90 PMMA 689/B34, (c) 15:85 PMMA 689/B34, (d) 20:80 PMMA 689/B34, and (e) neat PMMA 689.

DSC cannot be used to assess intercalation and the saturation ratios of PMMA to silicate as they can for semicrystalline PEO.[17] In that work, it was found that the same heat treatment of neat PEO, as used in the intercalation, did not change the degree of crystallinity, and so the strength of XRD peaks or melting endotherms in DSC could be used in nanocomposites to indicate the amount of nonintercalated polymer remaining outside the silicate gallery. We use the T_g values of materials remaining outside to indicate the saturation ratio, using DMTA and the *d*-spacing change in XRD.

DMTA results

DMTA was used to investigate the T_g values of the mixtures of the polymer and silicate before and after annealing and to provide confirmation of the values of the saturation ratio of PMMA to B34 determined by DSC.[12] Hydrostatically compressed disks of powders of neat PMMA 689, PMMA 424, and mixtures of PMMA and B34 were produced for testing by DMTA. The samples after annealing were used directly in the DMTA because they had previously been compressed into disks before annealing and conveniently remained in pellet form after melt intercalation. In plots of the loss modulus versus the temperature, the loss modulus is in arbitrary units because the penetration probe mode is not a true deformation mode and the values of the loss modulus are not absolute. However, the temperature location and shape of the curves are of interest. Essentially, the saturation level is determined from the composition of the silicate and polymer, at which T_g can be observed, deemed to be from the polymer remaining outside the galleries after annealing.

The results for PMMA 424 and PMMA 689 were the same in terms of the saturation ratio determined for B34, and so only data for PMMA 689 are shown as an example. Figure 4 shows a plot of the loss modulus versus the temperature for a series of physical mixtures of PMMA 689 and B34 of various concentration ratios before annealing, whereas Figure 5 shows a plot of the loss modulus versus the temperature for samples after annealing.

It is necessary to measure the data for hydrostatically compressed disks before annealing to determine at what composition the glass transition can be observed because of the dilution of the polymer phase and the sensitivity of the technique. It needs to be clearly demonstrated that any absence of a T_g peak for a sample is because it has been intercalated, not because its peak is not apparent for the experimental reasons mentioned previously. A small, broad peak suggestive of a T_g can be seen in samples of 5:95 and 10:90 PMMA 689/B34, but it is not very clear [Fig. 4 (a,b)]. However, in the samples with a PMMA 689 content of 15% or more [Fig. 4(c,d)], there is a clear peak indicating T_g of PMMA in the sample. Compared with the peak intensity of the neat PMMA 689 sample

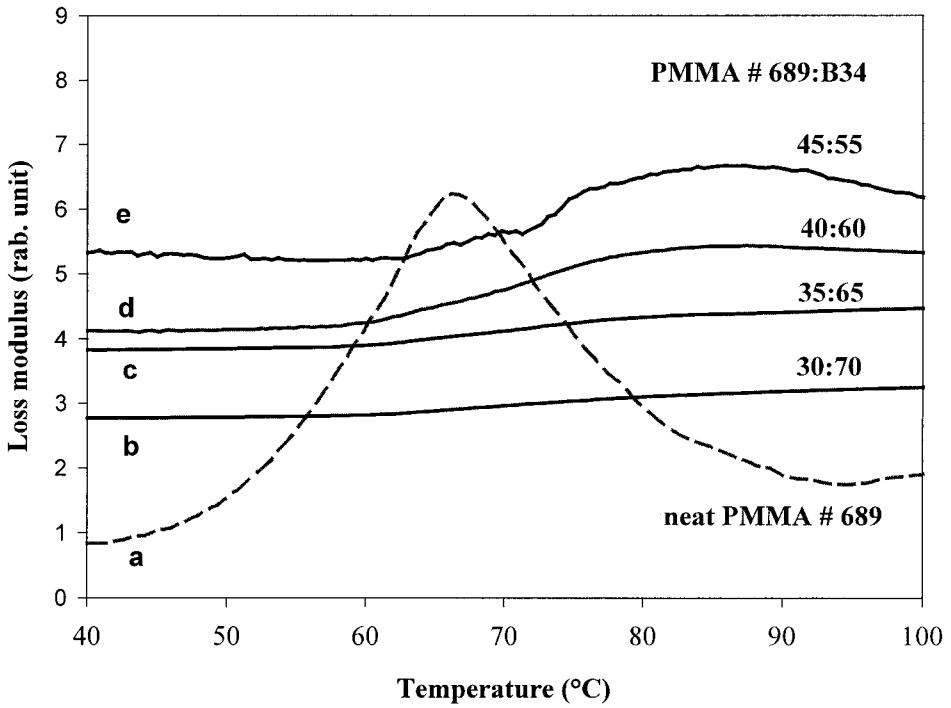

Figure 5 Loss modulus versus temperature for the PMMA 689/B34 system after annealing at 160°C for 8 h: (a) neat PMMA 689, (b) 30:70 PMMA 689/B34, (c) 35:65 PMMA 689/B34, (d) 40:60 PMMA 689/B34, and (e) 45:55 PMMA 689/B34.

in Figure 4(e), the intensity of the peak in the mixtures is much smaller. A PMMA content of 15% appears to be the base level required for a clear T_g to be observed by the DMTA technique. That is, in annealed samples, it is reasonable that only for samples with concentrations of the polymer greater than 15% could excess polymer outside the galleries be observed.

Figure 5(a) shows the curve for neat PMMA 689, indicating the peak position. No T_g is apparent in annealed samples with a PMMA 689 content of less than 35%, as shown in Figure 5(b,c). However, a peak indicative of T_g of PMMA 689 can be observed in the annealed samples with PMMA 689 contents of 40% or more, as shown in Figure 5(d,e). Because, as shown in the previous paragraph, a 15 wt % polymer concentration is required to be outside the gallery before it can be measured with the DMTA technique, we propose that the saturation ratio is 15% less than 40%; that is, at roughly 25%, the galleries are full, and 15% more is required before DMTA can see the peak. Thus, the saturation ratio of PMMA to B34 is approximately 25:75, as judged by this form of analysis.

Because the purpose of this section is to show the use of DMTA to determine the saturation ratio, another interesting finding, the DMTA peak appearing at higher temperatures than that of neat PMMA 689, is discussed later.

XRD results

XRD is also used as a tool to determine the saturation ratio through the examination of the appearance of the spectra as a function of the PMMA content after annealing. The annealed samples in the PMMA 424/B34 and PMMA 689/B34 systems were examined with XRD, and various PMMA/B34 ratios from 2:98 to 50:50 were used. Once again, the XRD patterns of the samples with PMMA 424 are very similar to those of the samples with PMMA 689. The values of the *d*-spacing of the (001) peak gradually increase from about 32.7 Å for PMMA 424 and 32.1 Å for PMMA 689 to about 36.8 Å when the PMMA content increases from 2 to 25%. The value then remains constant at about 36.8 Å for further increases in the PMMA content from 25 to 50%. This dependence of the *d*-spacing of the (001) and (002) peaks as a function of the PMMA content is shown in Figure 6.

When the PMMA content is only 2%, the increase in the gallery size in the PMMA/B34 hybrid is about 2 Å, and it gradually increases with increasing PMMA content. After the PMMA content reaches 25%, the gallery size remains the same, at a value of 6.8 Å for PMMA contents up to 50%. This could also imply that the saturation ratio of PMMA to B34 is about 25–30%. In addition, the *d*-spacing values of the (002) peaks in Figure 6 also make it clear that the gallery size gradually increases with the PMMA content up to about 30% and remains constant. Thus, even though the amorphous PMMA phase cannot be directly probed by XRD, the XRD results of clay-based spacing with the composition can supply evidence of the saturation ratio of PMMA to B34. The saturation ratio of PMMA melt intercalation into B34 has been deter-

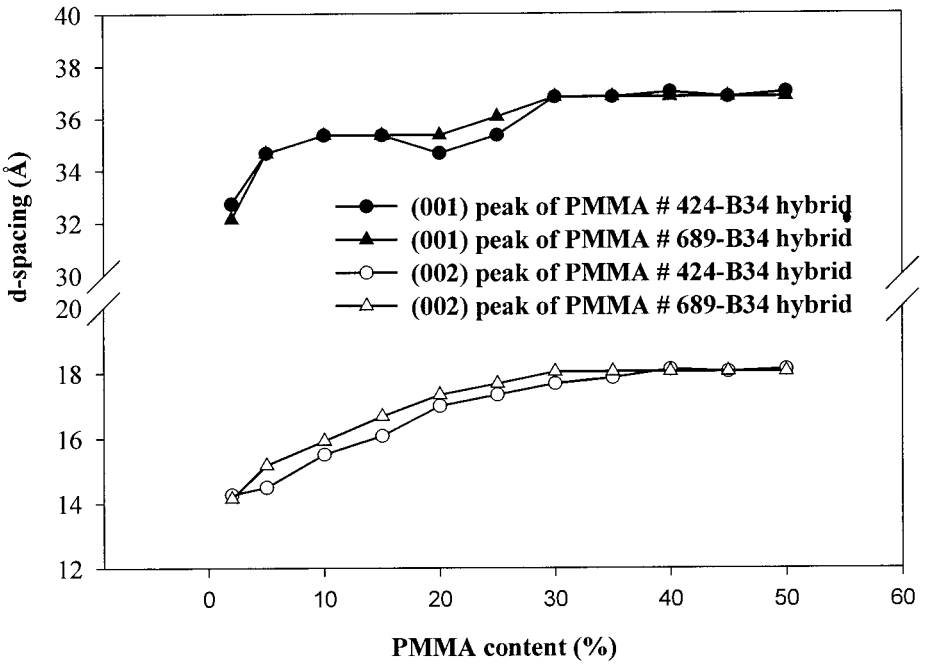

Figure 6 *d*-spacing of the (001) and (002) peaks of the PMMA/B34 hybrids for various PMMA contents in the PMMA 689/B34 and PMMA 424/B34 systems after annealing.

mined to be between 25 and 30% from DMTA and XRD results.

Moreover, these XRD results can also be used to obtain valuable information on the structure of PMMA/B34 hybrids. Note that the gradual increase in the gallery distance with the polymer content in the PMMA/B34 system is quite different from the one-step change of the gallery size in the PEO/silicate system.[16] The 6.8 Å expansion agrees well with that in a previously reported PMMA melt intercalation with B34.[18] An expansion of 5.8 Å was reported when the PMMA content was about 58.7% of a PMMA/MMT hybrid with emulsion polymerization,[8] whereas for a higher PMMA content, the interlayer distance was only about 3.5 Å.[8]

FTIR analysis

IR spectroscopy can be used to examine the manner in which the polymer chains are intercalated, restricted, or associated with the silicate. The details of the vibration bands and their assignments for the PMMA/B34 system are summarized in Table II.[19–27] Note that no IR analysis of B34 itself has been previously reported. Most of the assignments of the vibrations of silicate layers in B34 in Table II have been deduced from those assigned for MMT because they have very similar ceramic layers in their structures, although the vibration bands appear at slightly different positions. The presence of the characteristic group frequencies of both PMMA and B34 can be found together in the physical mixtures before annealing and in annealed hybrid samples, and most of these bands remain at the same location. This confirms the expected result that there are no strong forces between PMMA and B34 and that the confinement of PMMA in the B34 gallery occurs mainly by secondary forces, probably fairly weak in nature.

In the FTIR spectra of the intercalated samples, a shoulder appears around 1766 cm^{-1}, at a higher frequency than the band of the C═O (carbonyl) stretching (1738 cm^{-1}), and a new band appears at about 1800 cm^{-1}. The samples, which are not extensively intercalated, and the physical mixtures do not have such a shoulder or show a new band in their FTIR spectra. The FTIR spectra of the samples of 30:70 PMMA 424/B34 between 2000 and 1700 cm^{-1} are shown in Figure 7 for the purpose of comparing the band around 1738 cm^{-1} associated with C═O stretching. The band in the PMMA 424 intercalated hybrid located at 1738 cm^{-1} (C═O stretching) is split, and a shoulder at higher wave numbers around 1766 cm^{-1} is apparent. Note that a new band at about 1800 cm^{-1} can also be observed in the intercalated hybrid.

As mentioned previously, the band at 1738 cm^{-1} is clearly related to the C═O stretching mode. This band could be expected to shift to lower frequencies (lower wave number or larger wavelength) if existing dipolar bonding is disrupted. This has been explained, for example, in strongly hydrogen-bonded systems, in which there is a bond between a polar hydroxyl unit

TABLE II
IR Spectra for PMMA, B34, and the PMMA/B34 Hybrid (4000–400 cm^{-1})

Frequency (cm^{-1})	Frequency in reference (cm^{-1})	Assignment	Appearance in materials	Reference
3635	3624	ν(O—H)	B34, hybrid	19
3440	3420	ν(O—H)	B34, hybrid	20
3000	2995	$\nu(C—H)_a$	PMMA	21
2955	2956	$\nu((O)CH_3)$	PMMA, hybrid	22
2924–2930		$\nu(CH_2)_a$	B34→hybrid	23,24
2855–2868		$\nu(CH_2)_s$	B34→hybrid	23,24
1800			hybrid	
1766			hybrid	
1738	1736	ν(C═O)	PMMA	22
1638	1662, 1630	ν(C—O), ν (O—H)	B34, hybrid	25,26
1489	1485	$\delta(CH_3)_a$	PMMA	21
1452	1450	$\delta(CH_2)_a$,	PMMA	21
1440	1438	$\delta(CH_3—O)_a$	PMMA	21
1389–1393	1388	$\delta(CH_3)_s$	PMMA→hybrid	21
1276	1274	C(C═O)—O	PMMA, hybrid	22
1247	1245	C(C═O)—O	PMMA	22
1197	1196	C(C═O)—O	PMMA	22
1152	1155	C(C═O)—O	PMMA	22
1048–1044	1040	ν(Si—O)	B34→hybrid	27
992	996	$r(CH_3—O)$	PMMA	21
966	967	$r(CH_3)$	PMMA	21
755	759	$\nu(CH_3)$	PMMA	21
915, 884	915, 878	ν(Al—O—H)	B34, hybrid	20
846, 801	845–835, 796	ν[Al(Mg)—O—H]	B34, hybrid	20
527, 469	522, 467	ν[Al(Mg)—O—Si]	B34, hybrid	20

Mode assignments: ν (stretching); δ (bending); w (wagging); t (twisting); r (rocking). The subscripts a and s denote the asymmetric and symmetric motions with respect to the twofold axis perpendicular to the helix axis and passing through the O atom or the center of the C—C bond.

and a carbonyl group. It is proposed that if the secondary interaction is weakened, it reduces the bond stretch frequency because it deforms more easily, moving to lower wave numbers.[28] For example, a shoulder associated with the C═O bond in a system[28] in which there is a strong OH· · ·O═C interaction has been observed at a lower wave number near 1706 cm^{-1}. In this PMMA/B34 system, a split has been observed, but the shoulder band appears at a higher wave number. This may due to a stiffer C═O bond in the hybrid, resulting from weaker interactions between the carbonyl groups of the PMMA chains and the organic cations in comparison with interactions that exist between chains in the bulk PMMA state. This implies that there are interaction between the organochains in B34 and PMMA; even though they are very weak, they are sufficient to interfere with polar association between the PMMA chains. The presence of this new peak may be a further indication that PMMA has been intercalated into the silicate galleries and that the PMMA chains may have weak interactions with the organic chains of modified cations in the galleries of B34, which replace those between the PMMA chains after intercalation. Note that much of the driving force for intercalation is the increased entropy of the organoion chains as the clay moves apart,[13] and this counteracts the decrease in entropy due to polymer chain confinement.

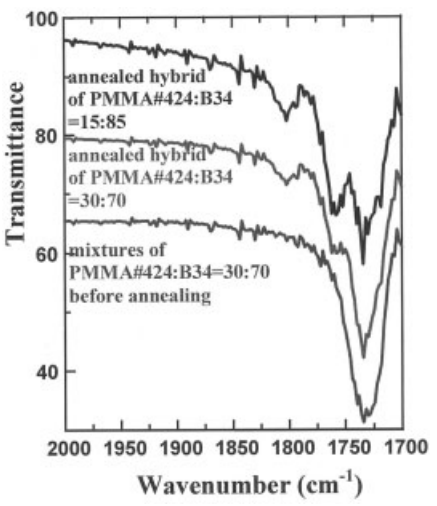

Figure 7 FTIR spectra between 3250 and 2750 cm^{-1} of the PMMA 689/B34 system with various ratios after annealing.

FTIR work was also performed by Lee and Jang[8] on the emulsion intercalation of a PMMA/MMT system and by Biasci et al.[27] on the *in situ* polymerization intercalation of MMA in the presence of functionalized MMT with 2-(*N*-methyl-*N*,*N*-diethylammonium iodide) ethyl acrylate (QD1) or 2-(*N*-butyl-*N*,*N*-diethylammonium bromide) ethyl acrylate (QD4) and hybrids of MMT with MMA/QD1 or MMA/QD4 copolymers. No evidence of new absorption bands (new secondary bonds) associated with interactions between organic and inorganic materials were reported in those works. We note that, for poly(butyl methacrylate), peaks can be observed in similar positions (1766 and 1800 cm^{-1}) related to enhanced anhydride formation in the presence of silica.[29] However, our work involves PMMA, and recent literature suggests that decomposition in PMMA is actually inhibited in the presence of the types of layered silicates used in this work and that the decomposition temperature increases by 15–120°C.

In summary, the FTIR spectra of the PMMA/B34 hybrids show evidence of weak interactions between PMMA and the organically modified cations, as well as PMMA intercalation into B34. A higher wave-number shoulder of the C═O stretching band and an unidentified band around 1800 cm^{-1} have been observed for the first time and may be due to the interaction of the PMMA chains and the organic chains of the modified cations in the galleries.

Thermal properties

Thermal degradation studies with TGA

TGA is a technique used to accurately track the *in situ* weight changes of a sample during a heating process, thereby providing information on thermal degradation. TGA has previously been applied to nanocomposites to differentiate between the mass of PEO remaining outside the hybrid and that contained within the silicate galleries.[17] It has been found that the polymer contained within the galleries is lost at higher temperatures because of the inhibition of degradation product mobility. In this way, the saturation ratio has been obtained for PEO intercalated into MMT. Most other polymers, including PMMA, require an organoion surface treatment for intercalation, and because this itself has a degradation process similar to that polymer, it interferes with the precise monitoring of the polymer degradation behavior. Because of the issue of overlapping PMMA and B34 degradations, the precise saturation ratio of PMMA to B34 cannot be deduced from TGA. TGA remains, however, a useful tool for determining changes in the degradation temperatures of samples.

The thermal and oxidative degradation of various types of PMMA have been extensively studied and fitted to various kinetic models[31] from thermogravimetric data in atmospheres of nitrogen and air.[32] If oxygen is in the atmosphere, the degradation becomes complex, depending on the method of PMMA synthesis. Oxygen has been found to enhance the degradation of anionically polymerized PMMA, whereas the effects of oxygen on the degradation of radically polymerized PMMA are much more complex.[32] The differential thermogravimetric analysis (DTG) results for anionically polymerized PMMA in both air and nitrogen show only one peak, and the temperature difference in the location of the DTG peak between the two atmospheres is about 50–60°C.[32] For radically polymerized PMMA, the important degradation mechanisms included depropagation, random main-chain scission, intramolecular or intermolecular transfer, and the scission of small molecules from side chains. The thermal degradation behavior depends on the experimental conditions, such as the heating rate, atmosphere, sample size, and geometry.[31] Two main reaction stages, which are reflected in two peaks in differential weight-loss curves (DTG), have been reported. The first reaction stage (200–300°C) is chain-end-initiated,[33] and the second (310–477°C) occurs by random scission.[34] PMMA chain connectively is almost completely destroyed at 450°C,[35] the primary degradation products being CO, CO_2, CH_3OH and CH_4.[36]

The DTG results for neat PMMA 424 and PMMA 689 show very similar curves in either air or nitrogen atmospheres, and the temperature difference for the DTG peak between the two atmospheres is 57°C. Figure 8 shows, as an example, the DTG curves of pure PMMA 424 in air and nitrogen atmospheres. There are two peaks at 334 and 427°C in the nitrogen atmosphere and at 275 and 370°C in air. Because the first peak is very weak, the main process observed in the PMMA samples studied would thus be higher temperature random scission.[34] The difference for the samples studied in air and nitrogen atmospheres is simply a shift in the temperature at which this primary mass loss occurs.

DTG results for the PMMA 424/B34 system are shown in Figure 9. Figure 9(a,b) shows the DTG curves of B34 and PMMA 424, respectively. The PMMA in the 20:80 PMMA 424/B34 physical mixture has the same temperature location as that of the neat PMMA 424 sample, as expected, both occurring at about 427°C. The physical mixture sample before annealing also shows an additional peak at a lower temperature (~378°C), which is associated with the decomposition of the alkyl ammonium ions in B34. The sample of the PMMA/B34 hybrid after annealing, however, has a peak at about 453°C, about 26°C higher than that of the pure PMMA sample and 75°C higher than that of pure B34. The intercalated hybrid does show a higher degradation temperature. It should be

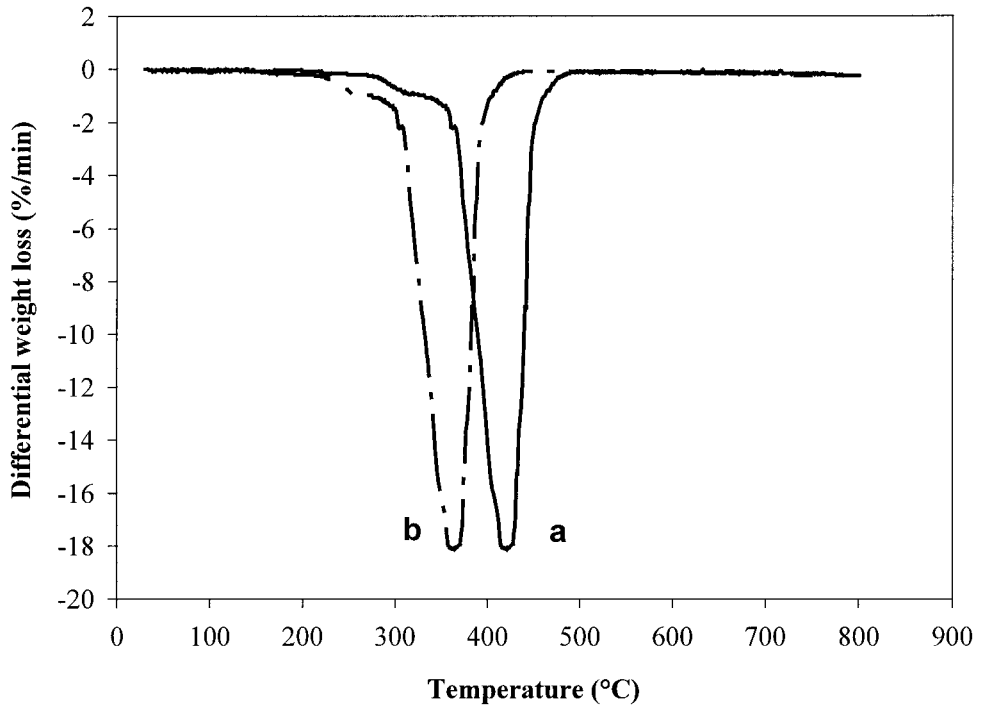

Figure 8 DTG curves of pure PMMA 424 (a) in a nitrogen atmosphere and (b) in air.

noted that some PMMA might intercalate into B34 during the TGA heating process. Fortunately, the samples used in TGA are loose powders, and the heating rate is fairly high, some 10°C/min, and so the time for such diffusion is limited.

T_g's

A glass-transition process of the polymer has not been observed for samples of the intercalated PMMA/B34 hybrid. An interesting phenomenon has been found in

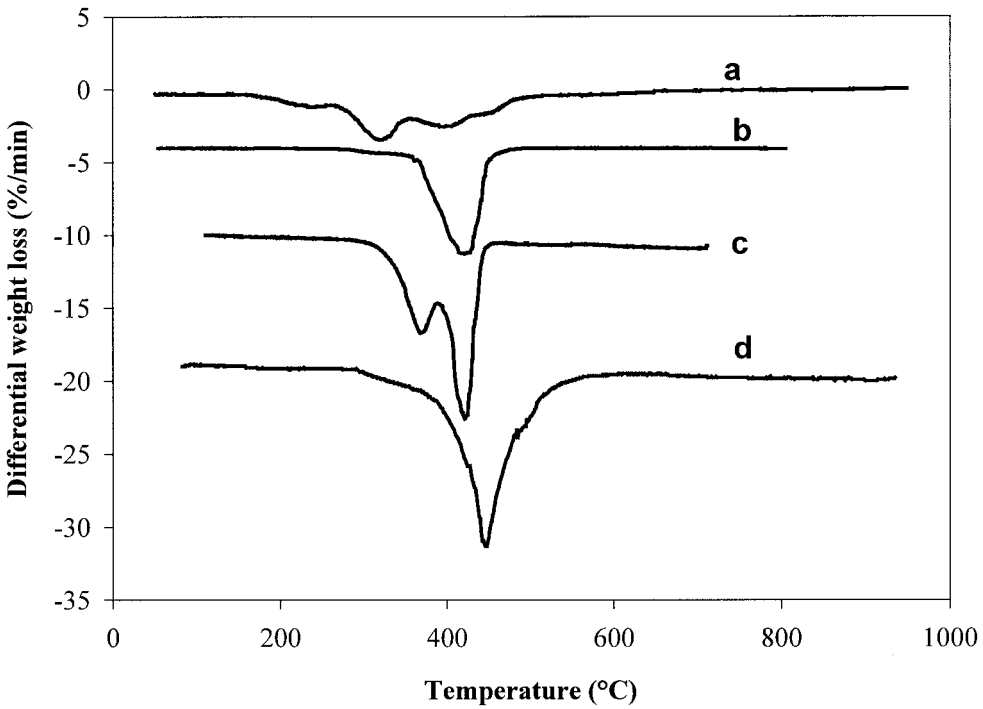

Figure 9 DTG curves for the PMMA 424/B34 system: (a) pure B34, (b) pure PMMA 424, (c) a 20:80 physical mixture of PMMA 424 and B34 before annealing, and (d) a 20:80 hybrid sample of PMMA 424 and B34 after annealing.

TABLE III
T_g Values of PMMA in Mixtures with B34 Before and After Annealing as Measured by DMTA

	PMMA content (%)					
	15	20	30	100	40[a]	45[a]
PMMA 424/B34	102	103	106	115	130	132
PMMA 689/B34	57	59	63	67	86	86

[a] Sample after annealing.

both the DSC and DMTA results. The DMTA results show that T_g of pure PMMA lies between that of an unannealed, physical mixture and that of a mixture with excess PMMA and B34 after annealing. Table III gives a summary of the glass-transition data from DMTA results, neat PMMA being included for comparison. Note that the saturation ratio of PMMA to B34 via melt intercalation is about 25:75. PMMA in a physical mixture at a 15 or 20% concentration would be very similar to excess PMMA in an annealed sample with a 40 or 45% concentration, respectively, after intercalation. The DSC results, however, show that T_g of pure PMMA is lower than that of a physical mixture before annealing and that T_g of the physical mixture before annealing is lower than that of a mixture with the hybrid after annealing. Table IV presents the T_g values of PMMA 424 and PMMA 689 as neat polymers and in physical polymer mixtures with B34 before annealing and with the PMMA/B34 hybrid after annealing, as determined by DSC.

A comparison of the values of T_g for neat PMMA and a physical mixture of the polymer and B34 before intercalation is necessary. In the DSC results, the physical mixture has a T_g about 6–9°C higher than that of neat PMMA. This can possibly be explained by the different heat capacities of the polymer and silicate. The heat capacities of PMMA and silicate at 25°C are about 1.42 kJ kg^{-1} K^{-1}[35] and 12.56 kJ kg^{-1} K^{-1},[37] respectively. DSC detects the difference in the electrical power supplies to the two sample holders, one containing the sample and another an empty reference, and measures it as a function of temperature and, therefore, the enthalpy change of the corresponding transition in the sample. The silicate in the mixture absorbs heat energy with less of a temperature change, and this causes a temperature lag and thus delays the detection and value of T_g. However, the result from DMTA is different. This T_g increase is likely related to the presence of silicate in the physical mixture, but a clear explanation is not available.

T_g of the PMMA in excess of the saturation ratio after intercalation increases in the same direction in both DSC and DMTA, although T_g of the PMMA in the physical mixtures changes in a different direction. For example, the T_g values of the polymer from the DSC and DMTA analysis of the sample with 40% PMMA 424 after annealing are 105 and 130°C, that is, 11 and 15°C higher than that of neat PMMA 424, respectively. T_g of the PMMA 689/B34 system increases by 12.5°C with DSC and by 19.0°C with DMTA.

The polymer material wholly confined within the silicate layers generally shows no contribution to the heat flow related to the glass transition of DSC and DMTA signals,[14] with only polymer outside the hybrid showing a T_g. However, if PMMA in the galleries has no effect on the excess PMMA outside the galleries, no change in T_g of the PMMA outside the hybrid after annealing (melt intercalation) should be expected. An increase of 12–19°C in T_g is observed with both DSC and DMTA. Such a T_g increase of about 10°C has also been found in a free-radical-polymerization PMMA matrix with exfoliated organically modified smectic clay,[7] and an increase of about 6°C has been found in emulsion-polymerization PMMA nanocomposites with exfoliated MMT.[9] The PMMA matrix with a filler of a PMMA-intercalated B34 hybrid has a higher increase of T_g than that with an exfoliated clay (either normal clay such as MMT or organically modified clay).

A possible explanation for the increase in T_g of the polymer outside the galleries could be the constraint on the molecular mobility of the polymer chains, which are at least partially confined between silicate layers. This partial intercalation could limit the mobility of the portion of the molecules that extend into the bulk region outside the clay. It is also possible that a given chain could tie the silicate platelets together by having both ends in different interlayer particles. Such a concept of reduced mobility and a resultant increase in T_g of the excess polymer could thus occur in the same way as increased crystallinity can lead to an increased T_g because of constraint. The silicate particles thus play the role of crystalline regions in the simplistic schematic model of semicrystalline polymers. Even if a chain is only constrained at one end because of intercalation, the immobility may still result in an increase in T_g of the external chains. A further possibility is that intercalation leads to a reduction in the polymeric free volume because the chain ends become located in silicate galleries, as this would also lead to an increase in T_g.

TABLE IV
T_g Values of PMMA in Mixtures with B34 Before and After Annealing as Measured by DSC

	PMMA content (%)					
	15	20	30	100	40[a]	45[a]
PMMA 424/B34	96	98	99	94	105	107
PMMA 689/B34	52	54	54	45	57	58

[a] Sample after annealing.

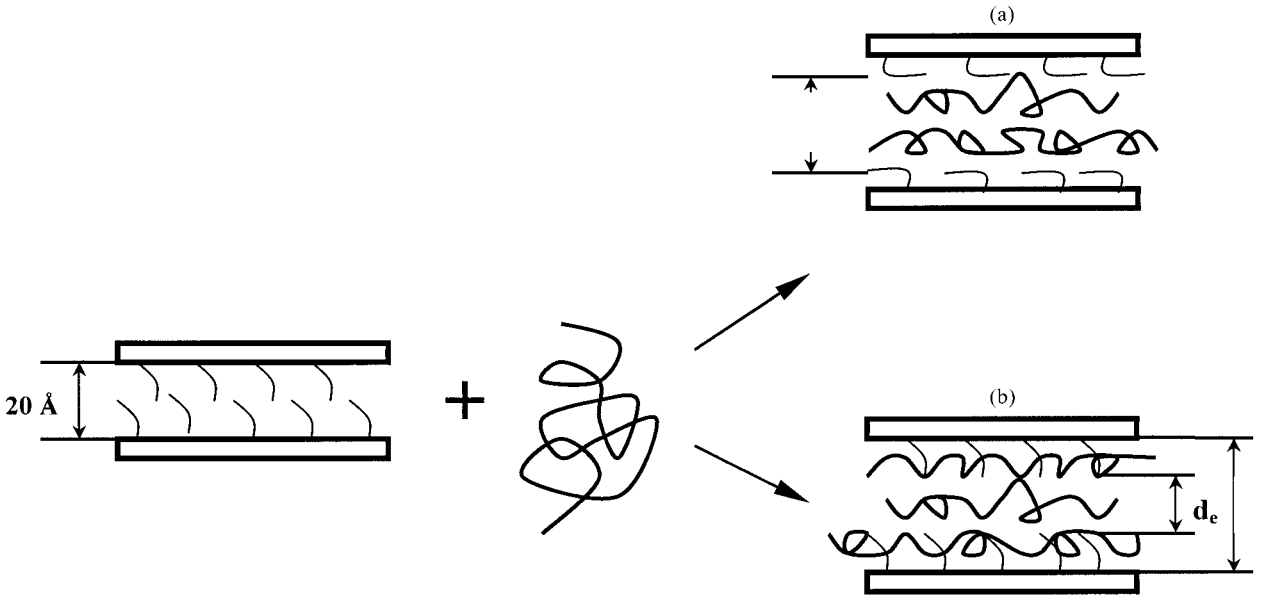

Figure 10 Schematic structural model of the PMMA/B34 hybrids: (a) PMMA chains largely occupy the empty space between the layers (d_e), in which organic chains densify and compress, and (b) the organic chains remain in a similar conformation, but PMMA chains are entangled within them and are able to directly interact with them, occupying the whole space between the ceramic layers (d_b).

Structural model

To propose a structural model of the PMMA/B34 nanocomposites, we used information in theoretical calculations with density data, FTIR, thermal analysis, and XRD.

We used the method in ref. 16 to calculate the size of a random coil of PMMA. The calculated values for PMMA 424 and PMMA 689 are 95 and 228 Å, respectively, with a value of characteristic ratio (C_∞) for atactic PMMA of 6.9.[38] However, the increase in the gallery size in the PMMA/B34 hybrids is only about 6.8 Å. The conformation of the chains cannot be coiled, and most exist as planar chains for PMMA in the B34 gallery; they are largely confined along the two-dimensional platelet directions.

The saturation ratio may be calculated according to the crystal lattice parameters of the silicate before and after intercalation.[16]

If the volume change (ΔV) is entirely caused by polymer occupation because of the intercalation (in other words, B34 does not change its density before and after intercalation), then the volume of the polymer (V_p) is equal to ΔV. Because the mass (M) is equal to $V\rho$ (where ρ is the density), the mass ratio (or weight ratio) of the polymer to B34 may be expressed as follows:

$$M_p/M_b = V_p\rho_p/V_b\rho_b = (ab\Delta c \sin \alpha\rho_p)/(abc \sin \alpha\rho_b) = (\Delta c\rho_p)/(c\rho_b) \quad (1)$$

where M_p and M_b are the masses of the polymer and B34, respectively; V_b is the volume of B34; and ρ_p and ρ_b are the densities of the polymer and B34, respectively. The densities of PMMA and B34 were measured to be 1.22 and 2.56 g/cm^3, respectively. The calculated value of the saturation ratio for the PMMA/B34 system is 14.6:85.4.

The theoretically calculated saturation ratio should be higher than that observed if the polymer density after intercalation is lower than that before intercalation. The aforementioned experimental results from DSC, DMTA, and XRD analysis of the saturation ratio indicate it may be too high (25:75). This must be due to one or more of the following: the conformation of the polymer or the organically modified chains in the gallery or an interaction between the PMMA and B34 layers in the PMMA/B34 system.

According to this experimental saturation ratio, the density of the polymer in the silicate gallery after intercalation (2.37 g/cm^3) will be much higher than that in the bulk polymer ($\sim$ 1.2 g/cm^3); this is unlikely. Because the ceramic layer itself cannot be changed during the annealing process of melt intercalation (at $<$250°C for 8 h), the only parameter that can possibly change is the effective nature of the gallery space of 20 Å occupied by the organic chains of the modified cations.

There are two possible ways that the gallery space changes to accommodate more polymer chains. Schematic structures outlining these two hypotheses are presented in Figure 10. One possibility is that organic

TABLE V
Empty Space that PMMA Requires (d_e) in the First Hypothesis and the Subsenquent Space for Modified Cations in the Gallery for 25:75 PMMA/B34

Density of PMMA (g/cm^3)	d_e (Å)	Space for modified cations (Å)
1.22	13.2	13.6
0.82	19.6	7.2

chains in the galleries are packed more closely to the surface of the silicate layer than those in pristine B34, leaving more space between the layers in which PMMA chains reside [Fig. 10 (a)]. Note that d_e is defined as the distance of the empty space between the organic chains in the gallery. The other possibility, shown in Figure 10(b), is that PMMA chains penetrate the whole space between the ceramic layers and intermix with the organically modified chains; d_b is defined as the distance between the ceramic layers. In the latter case, the PMMA chains interpenetrate the organic chains, whereas the organic chains retain approximately the same conformation as in nonintercalated B34.

The empty space that PMMA chains occupy in the first hypothesis [Fig. 10(a)] can be calculated if the density of PMMA in the gallery is known. The density of PMMA could be assumed to be between two extreme values for the further calculation for the PMMA/B34 system: 1.22 (in the bulk polymer) or 0.82 g/cm^3 (PEO in the PEO/B34 system previously reported[16]). Note that 0.82 g/cm^3 is only an approximate value in the PEO/B34 system. Table V shows the calculated distance of the empty space for PMMA (d_e) and the distance left for organic chains of B34 with the different assumed densities of PMMA. Note that 1.22 g/cm^3 is used as the average density of PMMA for simplicity of either PMMA 424 (1.21 g/cm^3) or PMMA 689 (1.23 g/cm^3) for the calculation in Table V. The ratio of PMMA to B34 used in the calculation is 25:75. Note that the density of B34 used in the calculation is 1.61 g/cm^3, although the organic chains (modified cations) occupy less space in the gallery after intercalation.

Comparing the calculated values of the remaining space for the organic chains of modified cations (7.2 or 13.6 Å) with the original space in B34, in which the organically modified cations are located (20 Å), we find that the change is large. The space that organically modified cations occupy is reduced by 12.8 or 6.4 Å when the density of the polymer is 0.82 or 1.22 g/cm^3, respectively. The reduction of the space for the organic chains is 64% if the density of PMMA in the gallery is assumed to be 0.82 g/cm^3 and about 32% even if the density is as high as that for the bulk polymer. This appears to rule out the first hypothesis, in which the organoion chains are pushed away by polymer chains from the center to the side of the interlayer galleries.

The empty space (d_e) of the second hypothesis [Fig. 10(b)] is the increase in the gallery size after intercalation obtained from the XRD analysis (6.8 Å). The total distance between the ceramic layers (d_b) after intercalation is 26.8 Å. The apparent density of PMMA remaining entangled within the organic chains of modified cations in B34 can thus be calculated with the saturation ratio. The value is about 0.24 g/cm^3, even if the density of PMMA in the empty space (d_e) is assumed to be that of the minimum value mentioned earlier, that of the polymer in the PEO/B34 system (0.82 g/cm^3). If the density of PMMA in the empty space is greater than 0.82 g/cm^3, the apparent density of PMMA intermixing with the organic chains of the modified cations will be smaller than 0.24 g/cm^3, and this seems reasonable. Moreover, comparing this hypothesis with the structure in the previous PEO/B34 system,[16] we find that the only difference is that PEO occupies the 6.8-Å gallery (or the empty space), whereas PMMA occupies both this space and the space among the organic chains of modified cations. This difference implies that PMMA has stronger interactions with the organic chains in B34 than PEO.

This concept of greater interaction and entanglement in the PMMA/B34 system is supported by the fact that there is an interaction between PMMA and the organically modified cations, as shown by FTIR analysis. Combined with the density considerations, the second hypothesis, in which polymer chains enter the whole interlayer gallery, including intermixing with the organoion chains, thus appears more likely for the PMMA/B34 system.

Thermal analyses further confirm the interactions of PMMA inside and outside the PMMA/B34 hybrid because an increase in T_g is observed and attributed to these interactions. A schematic structure of this hypothesis of the PMMA-intercalated B34 hybrid is shown in Figure 11. The PMMA chains occupy the B34 gallery, some of them close to and interacting with the organic chains of the cations, and some remaining in the empty space between the organic chains within the

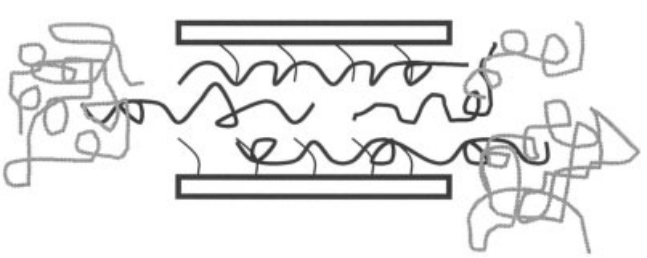

Figure 11 Schematic structure of excess PMMA and the PMMA/B34 hybrid. The grey lines represent excess PMMA outside the hybrid, which is in black.

gallery (d_e in Fig. 10). The conformation of PMMA is likely to be of an extended-chain nature along the length of the layers.

Furthermore, according to the XRD results, the gallery size (d_b in Fig. 10) of the hybrid increases from 20 Å in pristine B34 to 22–23 Å in a 2:98 PMMA/B34 hybrid and increases gradually with increasing PMMA loading in a sample to 26.8 Å in a 25:75 PMMA/B34 hybrid; it then remains consistent at about 26.8 Å with additional PMMA content. (Note that d_b is less than the d_{001} repeat distance because it does not include a 10-Å clay layer. Instead, d_b is the internal size of the gallery.) In other words, the gallery of B34 continues to be pushed apart gradually until an increase in the size of about 6.8 Å during PMMA intercalation. The half-height width of the (001) peak in the samples also suggests a distribution of interlayer spacings (gallery size). It suggests that the conformation and saturation of PMMA in the B34 gallery of PMMA/B34 hybrids are different from PEO intercalating into MMT or B34, in which the gallery distance does not change with the amount of PEO.[16]

The increases in the gallery size of MMT with methacrylate copolymer derivatives[27] vary between 4.7 and 20.1 Å, and that in the PMMA/MMT hybrid made by emulsion polymerization increases from 1.3 to 5.8 Å with the PMMA loading.[8] Along with the current findings, it can be concluded that the interlayer distance in PMMA/silicate hybrids varies with the PMMA content. The thickness increase predicted by the size of the MMA monomer cross-section diameter is about 6.4 Å,[8] which corresponds roughly to the gallery increase observed (the maximum increase in this study is ca. 6.8 Å). In the empty space of the fully intercalated hybrid (d_e = 6.8 Å), there seems to be one layer of PMMA planar chains, whereas there are some PMMA chains occupying the space among organic chains of the modified cations in both sides of the empty space. Sufficient evidence is not available to allow the determination of interlayer numbers per unit mass of silicate and the exact packing of PMMA in the gallery.

CONCLUSIONS

Evidence of melt intercalation for a low-molecular-weight atactic PMMA and a low-T_g isotactic PMMA into an organoion-treated bentonite, B34, was obtained with XRD, DSC, and FTIR techniques. The saturation ratio of PMMA to B34 was determined to be between 20 and 30 wt % polymer to layered silicate, as determined by XRD, DSC, and DMTA. The XRD results showed that the (001) *d*-spacing of the intercalated hybrid gradually increased with the PMMA content up to 25%, after which it plateaued off at about 36.8 Å.

The FTIR analysis yielded evidence of interactions between B34 and PMMA confined in the B34 gallery. Two new IR absorption bands were found in the PMMA/B34 hybrid. The one at about 1766 cm^{-1} may be a split of the C═O stretching (at 1738 cm^{-1}) and was likely due to reduced interactions of PMMA with itself because of increased association with the organic chains of modified cations in the B34 gallery.

The degradation temperature of PMMA in the hybrid was about 26°C higher than that of pure PMMA and 75°C higher than that of pure B34 according to TGA and DTG; the thermal stability of the PMMA/B34 hybrid nanocomposites was clearly enhanced. When excess PMMA was added to B34, T_g of the PMMA outside the hybrid gallery was found to be higher than that of neat PMMA, T_g increasing by about 12–19°C. The interaction of the PMMA chains outside the B34 gallery with those in the gallery (possibly straddling both regions) may be a possible explanation. A structural model was proposed based on different hypotheses and various experimental results. It is concluded that the PMMA chains occupy the B34 gallery, some penetrating and interacting with the organic chains of the modified cations.

References

1. Liu, L.; Qi, Z.; Zhu, X. J Appl Polym Sci 1999, 71, 1133.
2. Vaia, R. A.; Vasudevan, S.; Krawiec, W.; Scanlon, L. G.; Giannelis, E. P. Adv Mater 1995, 7, 154.
3. Vaia, R. A.; Ishii, H.; Giannelis, E. P. Chem Mater 1993, 5, 1694.
4. Chen, G.; Chen, X.; Lin, Z.; Ye, W. J Mater Sci Lett 2002, 18, 1761.
5. Hwu, J. M.; Jiang, G. J.; Gao, Z. M.; Xie, W.; Pan, W. P. J Appl Polym Sci 2002, 83, 1702.
6. Hirara, T.; Kashiwagi, T.; Brown, J. E. Macromolecules 1995, 18, 1410.
7. Okamoto, M.; Morita, S.; Taguchi, H.; Kim, Y. H.; Kotaka, T.; Tateyama, H. Polymer 2000, 41, 3887.
8. Lee, D. C.; Jang, L. W. J Appl Polym Sci 1996, 61, 1117.
9. Bandyopadhyay, S.; Giannelis, E. P. Proc Am Chem Soc Div Polym Mater: Sci Eng 2000, 82, 208.
10. Zhu, J.; Start, P.; Mauritz, K.; Kenneth, A.; Wilkie, C. A. Polym Degrad Stab 2002, 77, 253.
11. Du, J.; Zhu, J.; Wilkie, C. A.; Wang, J. Polym Degrad Stab 2002, 77, 377.
12. Shen, Z.; Simon, G. P.; Cheng, Y.-B. Mater Res Soc Symp Proc 1999, 576, 137.
13. Olson, B. G.; Peng, Z. L.; Srithawatpong, R.; McGervey, J. D.; Ishida, H.; Jamieson, A. M.; Manias, E.; Giannelis, E. P. Mater Sci Forum 1997, 255, 336.
14. Vaia, R. A.; Sauer, B. B.; Tse, O. K.; Giannelis, E. P. J Polym Sci Part B: Polym Phys 1997, 35, 59.
15. Shen, Z.; Simon, G. P.; Cheng, Y.-B. Polym Eng Sci 2002, 42, 2369.
16. Shen, Z.; Simon, G. P.; Cheng, Y.-B. Polymer 2002, 43, 4251.
17. Shen, Z.; Simon, G. P.; Cheng, Y.-B. Eur Polym J 2003, 39, 1917.
18. Vaia, R. A. Ph.D. Thesis, Cornell University, 1995.
19. Theng, B. K. G. Chemistry of Clay–Organic Reactions; Hilger: London, 1974.

20. van der Marel, H. W.; Beutelspacher, H. Atlas of Infrared Spectroscopy of Clay Minerals and Their Admixtures; Elsevier: Amsterdam, 1976; pp 31 and 113.
21. O'Reilly, J. M.; Mosher, R. A. Macromolecules 1981, 14, 602.
22. Sondag, A. H.; Raas, M. C. Polymer 1991, 32, 2917.
23. Papke, B. L.; Ratner, M. A.; Shriver, D. F. J Phys Chem Solids 1981, 42, 493.
24. Webb, S. W.; Stanley, D. A.; Scheiner, B. J. An Infrared Examination of Ion-Exchanged Montmorillonite Treated with Polyethylene Oxide; RI 9036; U.S. Bureau of Mines: Avondale, MD, 1986.
25. Tadokoro, H.; Chatani, Y.; Yoshihara, T.; Tahara, S.; Murahashi, S. Makromol Chem 1964, 73, 109.
26. Hummel, D. O. Atlas of Polymer Plastics Analysis, 3rd ed.; Hanser: Munich, 1991; Vol. 1, pp 258 and 460.
27. Biasci, L.; Aglietto, M.; Ruggeri, G.; Ciardelli, F. Polymer 1994, 35, 3296.
28. Coleman, M. M.; Graf, J. F.; Painter, P. C. Specific Interactions and the Miscibility of Polymer Blends: Practical Guides for Predicting and Designing Miscible Polymer Mixtures; Technomic: Lancaster, PA, 1991; p 221.
29. White, R. L.; Negelein, D. L. Am Lab 1998, 30, 33.
30. Huang, X. Y.; Brittain, W. J. Macromolecules 2001, 34, 3255.
31. Kashiwagi, T.; Inada, A.; Brown, J. E.; Hatada, K.; Kitayama, T.; Masuda, E. Macromolecules 1986, 19, 2160.
32. Solomon, D. H. J Macromol Sci Chem 1982, 17, 337.
33. Manring, L. E. Macromolecules 1991, 24, 3304.
34. Chang, T. C.; Liao, C. L.; Wu, K. H.; Wang, G. P.; Chiu, Y. S. J Polym Sci Part A: Polym Chem 1998, 36, 2521.
35. Kashiwagi, T.; Inada, A.; Hamins, A. Polym Degrad Stab 1989, 26, 161.
36. Wunderlich, W. In Polymer Handbook, 3rd ed.; Brandrup, J.; Immergut, E. H., Eds.; Wiley-Interscience: New York, 1989; Chapter 5, p 78.
37. Cowie, J. M. G. Eur Polym J 1975, 11, 297.
38. Strobl, G. The Physics of Polymers; Springer: Heidelberg, 1996; Chapter 2.